Palladium Nanoparticles as Catalysts for Li-O_2 Battery Cathodes

Hugh Geaney,[1,2] Gillian Collins,[1,2,3] Colm Glynn,[1,2] Justin D. Holmes[1,2,3], and Colm O'Dwyer[1,2*]

[a] Department of Chemistry, University College Cork, Cork, Ireland
[b] Micro & Nanoelectronics Centre, Tyndall National Institute, Lee Maltings, Cork, Ireland
[c] Centre for Research on Adaptive Nanostructures and Nanodevices (CRANN), Trinity College Dublin, Dublin 2, Ireland

This report investigates the influence of electrolyte selection and the addition of Pd nanoparticle catalysts on the morphology of discharge products for Li-O_2 battery cathodes. Super P carbon cathodes (on stainless steel current collectors) were subjected to single discharges at various applied currents (50 µA, 100 µA, 250 µA) using either a sulfolane/LiTFSI or TEGDME/LITFSI electrolyte. The morphologies of the discharge product were noted to be different for each electrolyte while there was also a clear variation with respect to applied current. Finally, the impact of adding 25% (by weight) Pd nanoparticle catalysts to the cathodes was investigated. The results obtained show clearly that the nature of discharge products for Li-O_2 battery cathodes are strongly dependent on applied current, electrolyte choice and the addition of a catalyst material.

Introduction

Li-O_2 batteries have attracted recent research interest owing to their potential for outperforming current Li-ion technologies and thus finally making electric vehicles a practical alternative to those relying on combustion engines.(1) Energy storage within Li-O_2 batteries occurs *via* fundamentally different processes to those employed within Li-ion batteries. The most widely accepted pathway for Li-O_2 battery operation is through the reversible formation/decomposition of Li_2O_2 upon the cathode surface during discharge and charge respectively.(2) This battery chemistry boasts an exceptional theoretical capacity of 3505 $Whkg^{-1}$, however, greater understanding of the fundamental mechanisms underpinning discharge and charge and advances in Li-O_2 battery components (particularly the cathode and electrolyte) are required if the potential of Li-O_2 batteries is to be fully realized.(3) One of the key issues facing Li-O_2 batteries is the formation of parasitic byproducts on the cathode surface. Species such as Li_2CO_3, LiOH and HCO_2Li can be formed through decomposition of either the electrolyte or the cathode itself with accumulation of these products ultimately leading to battery failure.(4, 5) Stability issues with commonly used, carbonate based Li-ion electrolytes within Li-O_2 architectures (which readily form Li_2CO_3 even from the first discharge) have necessitated investigations into electrolytes which are resistant to reaction with Li_2O_2 (and its intermediate forms) and are also stable with respect to the wide potential windows required for LiO_2 battery operation. To date, a number of more stable alternative electrolyte solvents such as tetraethylene glycol dimethyl ether (TEGDME)(6) and

sulfolane(7) have been identified as more suitable replacements to carbonate based electrolytes but need to be probed further if they are to be viable electrolyte solvents in future.

Various types of commercial carbon (e.g. Super P and Vulcan XC72 among others) have been investigated as cathode materials for Li-O_2 applications due to their low cost, low densities (which facilitate high gravimetric capacities) and high surface areas.(8) Surface area in particular is an important consideration as the capacity of any Li-O_2 cell is directly related to the amount of Li_2O_2 that can be accommodated on the cathode. Recently, increasing attention has been devoted to understanding the way in which Li_2O_2 forms on the cathode surface.(9-11) Ex-situ analyses of various carbon cathodes have shown evidence of various morphological forms of Li_2O_2, varying from films to spheres and more complex toroids after single discharges.(12-14) The shape, size and crystallinity of Li_2O_2 on the cathodes has also been found to be intrinsically linked to the discharge capacity and also significantly influence the recharge behavior of the cell (i.e. Li_2O_2 decomposition).(14) Furthermore, the morphology and crystallinity of Li_2O_2 formed on Super P cathodes has also been found to be dependent upon the applied current. Nazar et al. showed that crystalline Li_2O_2 toroids proliferate the cathode surface after discharge at low current densities, while at higher current densities, largely amorphous Li_2O_2 films were formed.(13)

Various metal and metal oxide nanostructures have been employed as catalysts in an effort to improve the round trip efficiency, rate capability and capacity of Li-O_2 batteries.(15) Ideally, catalysts should be bi-functional with respect to the oxygen reduction reaction (ORR) and oxygen evolution (OER) reaction associated with discharge and charge respectively. Of the various catalyst systems that have attracted attention, the most promising appear to be precious metal catalysts such as Au,(2, 16) Pd(17-20) and Pt(16) and metal oxides such as MnO_2(21-27) and Co_3O_4.(28, 29) While these catalyst materials have all shown promise as catalyst materials for Li-O_2 battery cathodes (usually in the form of increased charge capacity and reduced OER voltages compared to pure carbon cathode analogues), greater understanding of their mode of action is required. In contrast to the aforementioned ex-situ studies performed on carbon cathodes to gauge the formation and decomposition of Li_2O_2 during battery operation, little information is known of the formation of Li_2O_2 on catalytic systems.

In this study we have investigated the morphology of the discharge products formed on Super P carbon Li-O_2 battery cathodes at three different applied currents (250 μA, 100 μA and 50 μA) within TEGDME and sulfolane based electrolytes. This data was then compared with that obtained for cathodes containing 25% (by weight) Pd nanoparticle catalysts in an attempt to quantify the impact of the Pd nanoparticles on the morphology of the discharge products within the two electrolytes. These results confirmed a difference in the morphology of the discharge products on the cathodes as a function of the applied current but also illustrated that the morphology of the discharge products is also influenced by the electrolyte used and the incorporation of a catalyst material.

Experimental

Materials

Super P carbon, Li chips and stainless steel meshes were purchased from MTI Corporation USA. Sulfolane (99%), TEGDME, Bis(trifluoromethane) sulfonimide lithium salt (LiTFSI) and PVDF binder were purchased from Aldrich and used as received.

Pd Nanocrystal Synthesis

Cubic nanocrystals used in this study were prepared according to a published procedure.(30) Briefly, for the synthesis of 20 nm cubic Pd nanocrystals, 105 mg of PVP (Mw ~ 55,000), 60 mg of ascorbic acid and 600 mg of KBr were dissolved in 8 ml of water. The solution was heated for 10 min at 80 °C, under stirring followed by addition of 57 mg Na_2PdCl_4 dissolved in 3 ml of water. The solution was heated to 80 °C and aged for 3 h after which the product was collected by centrifugation, washed with water and briefly sonicated. This purification procedure was repeated 3 times before re-dispersing the nanocrystals in 10 ml of distilled water.

Preparation of cathodes

All of the cathodes studied were prepared using stainless steel mesh current collector disks from MTI (diameter 1.5 cm, area 1.76 cm^2). All of the active materials investigated were first made up as slurries (with or without binder as specified below) before being dip-coated on to the current collector. Super P slurries were prepared by mixing Super P carbon, PVDF binder and NMP (80:20 weights respectively for the solids). All cathodes were dried in an oven overnight at 100 °C to evaporate the NMP solvent and were immediately transferred in to an Ar filled glovebox where they were stored before analysis. Given the importance of mass loading to the operation of Li-O_2 cathodes,(13, 31) the active mass in each case was controlled between 1.4 ± 0.2 mg per cathode unless otherwise stated. As a result, the applied current rate of 100 mAg^{-1} equated to an applied current of 140 ± 20 μA.

Li-O_2 cell assembly and testing

Li-O_2 testing was conducted within an EL-Cell split cell. All cells were constructed within an Ar filled glovebox. Carbon cathodes were first placed on the metal separator. A glass fiber filter paper was used as separator upon which 100 μl of electrolyte (1M LiTFSI in sulfolane or TEGDME) was placed. A Li chip (MTI) was scraped on both sides to remove protective coating and used as the anode. The cell was tightened and removed from the glovebox where it was immediately connected to an O_2 line and was purged with 0.25 bar O_2 for 60 minutes at open circuit voltage (OCV). Following this period, electrochemical measurements were conducted using a VSP Biologic galvanostat. For constant current experiments, the applied current was calculated based on the entire mass of material on the current collector. All voltages quoted are vs Li/Li+.

Material characterisation

SEM analysis was performed on an FEI Quanta 650 FEG high resolution SEM equipped with an Oxford Instruments X-MAX 20 large area Si diffused EDX detector. Images were collected at an operating voltage of 10-20 kV. All cathodes for SEM analysis were stored in an Ar filled glovebox and transferred in closed containers with 0.1 ppm H_2O and O_2. Samples were loaded into the SEM as rapidly as possible (with an air exposure of <20 seconds) as previously reported by others.(32) TEM analysis was conducted using a JEOL 2100 high resolution TEM with a LaB_6 electron source.

Results and discussion

Super P carbon cathodes

Single discharges were conducted on Super P carbon cathodes within a Li-O_2 configuration as described in the experimental section. Parallel tests were conducted using electrolytes based on sulfolane and TEGDME to investigate the influence of the electrolyte solvent on the morphology of the discharge products. The SEM images presented in Figure 1 (a-c) show the nature of the discharge products formed on Super P cathodes at applied currents of 50, 100 and 250 µA using a 1M LiTFSI/sulfolane electrolyte system. It can be seen that the discharge products vary from individual characteristic Li_2O_2 toroids(12) at an applied current of 250 µA to fused aspherical particles at 100 µA and finally to much larger sheets >10 µm in size at 50 µA.

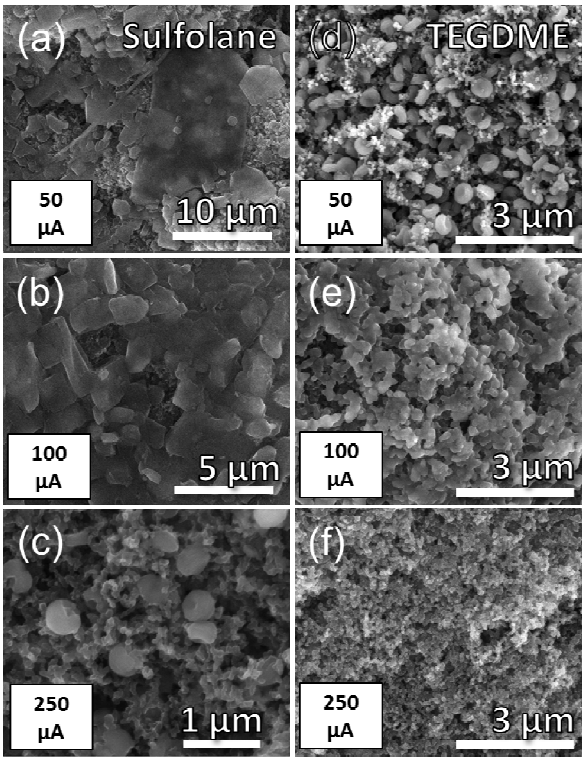

Figure 1: SEM images of pure Super P carbon cathodes which have been subjected to single discharges at the indicated applied currents. a-c) Cathodes discharged in sulfolane/LiTFSI at 50,100 and 250 µA. d-f) Cathodes discharged in TEGDME/LiTFSI at 50,100 and 250 µA.

In contrast, the morphology of the discharge products formed on the cathodes discharged using a TEGDME/LiTFSI electrolyte are shown in the SEM images in Figure 1 (d-f). For the cathode discharged at 50 µA (Figure 1 d), toroid formation across the surface of the cathode surface can clearly be seen which is markedly different to that exhibited by the Super P cathode discharged in the sulfolane electrolyte. For the cathode discharged at 100 µA, there is evidence of a film formation (similar to that observed for the corresponding current for sulfolane) on the cathode. The cathode discharged at 250 µA showed no clear evidence of discharge product formation which is likely due to the rapid discharge (<1 hr) exhibited by this cathode. It should be noted that the morphologies of the discharge product for the TEGDME electrolyte here are similar to those previously reported at similar current densities by Nazar et al. which is logical as their study focused on a TEGDME/LiTFSI electrolyte and also used a Super P carbon based cathode.(13) Thus, we can attribute variations in the morphology of the discharge products in Figure 1 ((a-c compared with d-f)) to the impact of the electrolyte solvent. Future studies will investigate the nature of discharge products in other electrolyte solvents and using alternative electrolyte salts.

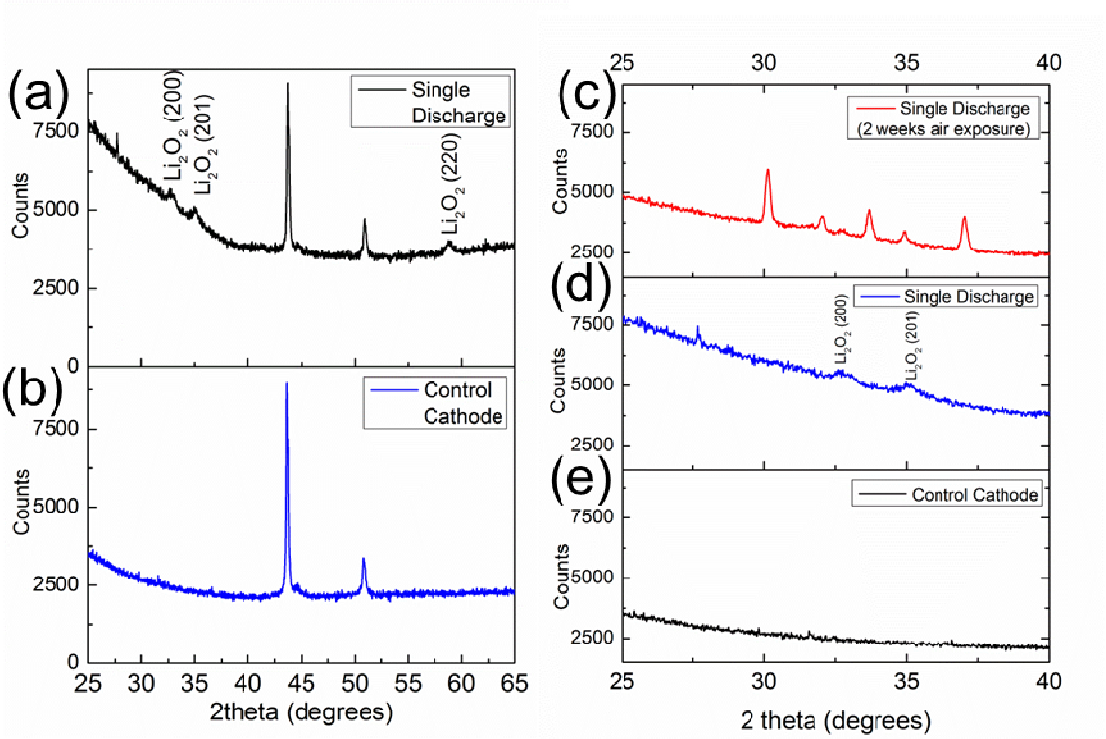

Figure 2: a) XRD analysis performed on a) Super P cathode after a single discharge (discharged with an applied current of 100 µA) with the indexed reflections indicating the presence of crystalline Li_2O_2 b) control Super P cathode. c-e) show narrower regions of the diffractograms for the control cathode (e), single discharge cathode (d) and the same discharged cathode left in ambient conditions for 2 weeks (c).

XRD analysis was performed on a cathode discharged within sulfolane/LITFSI electrolyte at 100 µA in an effort to identify the crystalline constituents of the discharge products. When comparing the discharged cathode (Figure 2a) with the pristine cathode (Figure 2 b), clear, broad reflections consistent with the formation of crystalline Li_2O_2 on the cathode surface can be identified. While this analysis illustrates the formation of

Li_2O_2 as the dominant crystalline discharge product, it must be noted that it does not account for any possible amorphous byproducts. Analytical techniques such as solid state ^{7}Li and ^{17}O or Raman scattering spectroscopy are better placed to identify the various constituents (both crystalline and amorphous) of discharged Li-O_2 battery cathodes and will be probed in future.(2, 33)

The cathode was stored in ambient conditions for 2 weeks to investigate the stability of the discharge products. In Figure 2 (c) it can be seen that after 2 weeks, the broad crystalline reflections consistent with the presence of Li_2O_2 on the cathode surface directly after discharge (Figure 2 d) have been replaced with much sharper reflections which are consistent with the conversion of the discharge product to $LiOH.H_2O$.

25% weight Pd/carbon cathodes

Having determined that the morphology of the discharge products relies on the electrolyte solvent and the applied current, the influence of the addition of 25% weight of 20 nm Pd nanoparticles to the cathodes was examined. Cathodes were prepared by adding Pd nanoparticles to the cathode slurry and were mixed overnight to ensure homogenous distribution within the carbon. Figure 3 a) shows a low magnification TEM image where Pd nanocubes can clearly identified throughout the supporting amorphous Super P carbon. The shape of the nanocubes and their crystallinity is confirmed by the high resolution TEM image in Figure 3 (b).

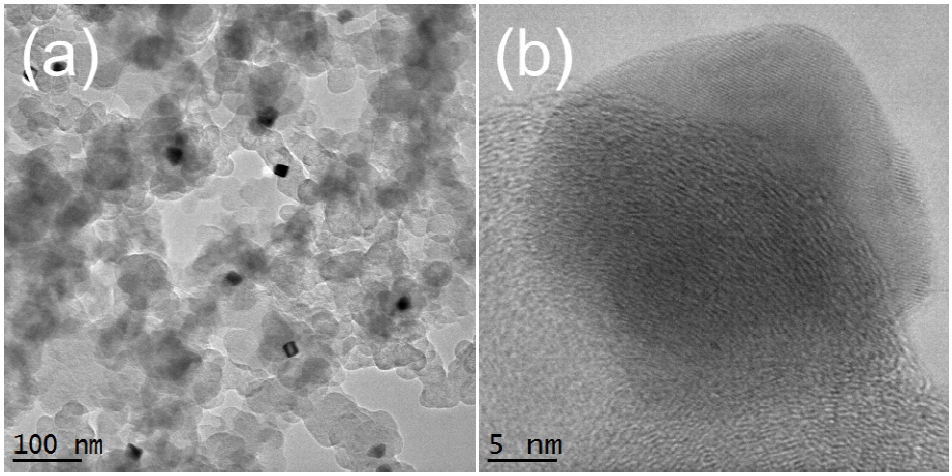

Figure 3: TEM images of Pd nanocubes on Super P carbon.

The SEM images in Figure 4 show the morphology of the discharge products formed on the 25% Pd cathodes at the same applied currents as those investigated for the pure Super P cathodes in Figure 2. For the cathode discharged at 50 µA (Figure 4a) the discharge products present as characteristic Li_2O_2 toroids which differs from the widespread film formation noted for the corresponding discharge using the sulfolane electrolyte. In the case of the cathode discharged at 100 µA (Figure 4b), large particles were noted across the cathode surface which again is different from the widespread fused toroids and particles observed for the sulfolane discharge. Finally, the toroidal morphology noted for the sulfolane cathode at an applied current of 250 µA was also seen for the TEGDME cathode (Figure 4c).

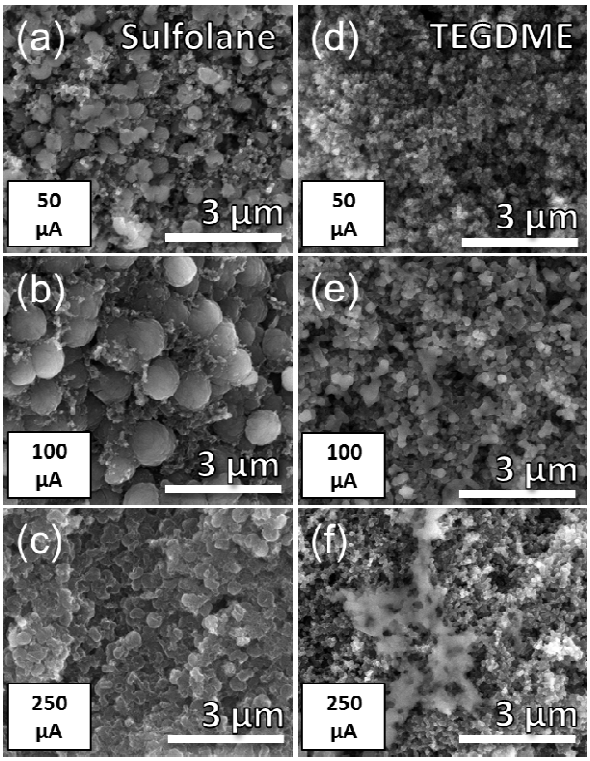

Figure 4: SEM images of 25% Pd cathodes after single discharges at the indicated applied currents. a-c) Cathodes discharged in sulfolane/LiTFSI at 50-250 µA. d-f) Cathodes discharged in TEGDME/LiTFSI at 50-250 µA

Single discharges were also carried out for the 25% Pd cathodes in the TEGDME electrolyte. From Figure 4, it can be seen that the morphology of the discharge products (Figure 4 (d-f)) vary strongly from those evident for the sulfolane cathodes (Figure 4 (a-c)). In comparison to the pure Super P cathodes discharged in sulfolane, there are no toroids evident when discharged at 50 µA, while a similar film formation to that noted for the pure Super P sample is observed for the 100 µA cathode. For the sample discharged at 250 µA it can be seen that there is sporadic film formation present for the 25% Pd sample which contrasts with the lack of obvious discharge product formation for the corresponding pure Super P carbon cathode. From the results presented in Figure 4, it can be seen that the introduction of Pd nanoparticles influences the morphology of the discharge products for Li-O_2, however there is also a large variation between different electrolytes and currents. This suggests that the formation mechanism for Li_2O_2 on carbon based cathodes is extremely sensitive to various experimental parameters. Further studies will focus on cathodes with different Pd weight percentages, additional applied currents and alternative catalyst materials. Understanding the decomposition processes for the various morphologies and their reformation are also key issues if a rechargeable system is to be realized.

Conclusions

In conclusion, we have investigated the impact of electrolyte, applied current and the addition of 25% Pd nanoparticle catalysts on the morphology of the discharge products formed on Li-O_2 battery cathodes. It was found that the nature of Li_2O_2 formed on the cathodes was strongly influenced by the electrolyte used, the applied current and also the addition of Pd catalysts. This report highlights the importance of investigating the impact of multiple parameters on the operation of Li-O_2 batteries. Such investigations will expand the understanding of the operation of Li-O_2 batteries towards rechargeable systems.

Acknowledgments

This research has received funding from the Seventh Framework Programme FP7/2007-2013 (Project STABLE) under grant agreement n°314508.

References

1. P. G. Bruce, S. A. Freunberger, L. J. Hardwick and J. M. Tarascon, *Nature Mater.*, **11**, 19 (2011).
2. Z. Peng, S. A. Freunberger, Y. Chen and P. G. Bruce, *Science*, **337**, 563 (2012).
3. Y. Shao, F. Ding, J. Xiao, J. Zhang, W. Xu, S. Park, J.-G. Zhang, Y. Wang and J. Liu, *Adv. Funct. Mater.*, **23**, 987 (2012).
4. S. A. Freunberger, Y. Chen, Z. Peng, J. M. Griffin, L. J. Hardwick, F. Bardé, P. Novák and P. G. Bruce, *J. Am. Chem. Soc.*, **133**, 8040 (2011).
5. M. M. Ottakam Thotiyl, S. A. Freunberger, Z. Peng and P. G. Bruce, *J. Am. Chem. Soc.*, **135**, 494 (2012).
6. C. Laoire, S. Mukerjee, E. J. Plichta, M. A. Hendrickson and K. Abraham, *J. Electrochem. Soc.*, **158**, A302 (2011).
7. D. Xu, Z.-l. Wang, J.-j. Xu, L.-l. Zhang, L.-m. Wang and X.-b. Zhang, *Chem. Commun.*, **48**, 11674 (2012).
8. Y. Zhang, H. Zhang, J. Li, M. Wang, H. Nie and F. Zhang, *J. Power Sources*, **240**, 390 (2013).
9. H.-G. Jung, H.-S. Kim, J.-B. Park, I.-H. Oh, J. Hassoun, C. S. Yoon, B. Scrosati and Y.-K. Sun, *Nano Lett.*, **12**, 4333 (2012).
10. J.-B. Park, J. Hassoun, H.-G. Jung, H.-S. Kim, C. S. Yoon, I. Oh, B. Scrosati and Y.-K. Sun, *Nano Lett.*, **13**, 2971 (2013).
11. L. Zhong, R. R. Mitchell, Y. Liu, B. M. Gallant, C. V. Thompson, J. Y. Huang, S. X. Mao and Y. Shao-Horn, *Nano Lett.*, **13**, 2209 (2013).
12. R. R. Mitchell, B. M. Gallant, Y. Shao-Horn and C. V. Thompson, *J. Phys. Chem. Lett.*, 1060 (2013).
13. L. Nazar, B. Adams, R. Black, C. Radtke, K. Zaghib and M. Trudeau, *Energy Environ. Sci.*, **6**, 1772 (2013).
14. B. M. Gallant, D. G. Kwabi, R. R. Mitchell, J. Zhou, C. Thompson and Y. Shao-Horn, *Energy Environ. Sci.*, **6**, 2518 (2013).
15. Y. Shao, S. Park, J. Xiao, J.-G. Zhang, Y. Wang and J. Liu, *ACS Catal.*, **2**, 844 (2012).
16. J. Zhang, G. Chen, M. An and P. Wang, *Int. J. Electrochem. Sci*, **7**, 11957 (2012).

17. D. Zhu, L. Zhang, M. Song, X. Wang and Y. Chen, *Chemical Commun.*, **49**, 9573 (2013).
18. A. K. Thapa, K. Saimen and T. Ishihara, *Electrochem. Solid St.*., **13**, A165 (2010).
19. A. K. Thapa and T. Ishihara, *J. Power Sources*, **196**, 7016 (2011).
20. J. Lu, Y. Lei, K. C. Lau, X. Luo, P. Du, J. Wen, R. S. Assary, U. Das, D. J. Miller and J. W. Elam, *Nature Commun.*, **4** (2013).
21. T. T. Truong, Y. Liu, Y. Ren, L. Trahey and Y. Sun, *ACS Nano*, **6**, 8067 (2012).
22. J. Li, N. Wang, Y. Zhao, Y. Ding and L. Guan, *Electrochem. Commun.*, **13**, 698 (2011).
23. Y. Cao, Z. Wei, J. He, J. Zang, Q. Zhang, M. Zheng and Q. Dong, *Energy Environ. Sci.*, **5**, 9765 (2012).
24. Y. Qin, J. Lu, P. Du, Z. Chen, Y. Ren, T. Wu, J. T. Miller, J. Wen, D. J. Miller, Z. Zhang and K. Amine, *Energy Environ. Sci.*, **6**, 519 (2013).
25. H. W. Park, D. U. Lee, L. F. Nazar and Z. Chen, *J. Electrochem. Soc.*, **160**, A344 (2013).
26. G. Zhang, J. Zheng, R. Liang, C. Zhang, B. Wang, M. Au, M. Hendrickson and E. Plichta, *J. Electrochem. Soc.*, **158**, A822 (2011).
27. K.-S. Song, J. Jung, Y. U. Heo, Y. C. Lee, K. Cho and Y. Kang, *Phys. Chem. Chem. Phys.*, **15**, 20075 (2013).
28. Z. Ren, Y. Guo, Z. Zhang, C. Liu and P.-X. Gao, *J. Mater. Chem. A*, **1**, 9897 (2013).
29. A. Riaz, K.-N. Jung, W. Chang, S.-B. Lee, T.-H. Lim, S.-J. Park, R.-H. Song, S. Yoon, K.-H. Shin and J.-W. Lee, *Chemical Commun.*,**49**,5984 (2013).
30. M. Jin, H. Zhang, Z. Xie and Y. Xia, *Angew. Chem. Int. Ed.*, **50**, 7850 (2011).
31. S. Beattie, D. Manolescu and S. Blair, *J. Electrochem. Soc.*, **156**, A44 (2009).
32. M. J. Trahan, Q. Jia, S. Mukerjee, E. J. Plichta, M. A. Hendrickson and K. Abraham, *J. Electrochem. Soc.*, **160**, A1577 (2013).
33. M. Leskes, N. E. Drewett, L. J. Hardwick, P. G. Bruce, G. R. Goward and C. P. Grey, *Angew. Chem. Int. Ed.*, **51**, 8560 (2012).